Steel and Composite Structures, *Vol. 19, No. 5 (2015) 1055-1075*
DOI: http://dx.doi.org/10.12989/scs.2015.19.5.1055

Application of steel equivalent constitutive model for predicting seismic behavior of steel frame

Meng Wang [*1] Yongjiu Shi [2a] and Yuanqing Wang [2b]

[1] *School of Civil Engineering, Beijing Jiaotong University, Beijing 100044, China*
[2] *Department of Civil Engineering, Tsinghua University, Beijing 100084, China*

(*Received February 16, 2014, Revised September 29, 2014, Accepted June 24, 2015*)

Abstract. In order to investigate the accuracy and applicability of steel equivalent constitutive model, the calculated results were compared with typical tests of steel frames under static and dynamic loading patterns firstly. Secondly, four widely used models for time history analysis of steel frames were compared to discuss the applicability and efficiency of different methods, including shell element model, multi-scale model, equivalent constitutive model (ECM) and traditional beam element model (especially bilinear model). Four-story steel frame models of above-mentioned finite element methods were established. The structural deformation, failure modes and the computational efficiency of different models were compared. Finally, the equivalent constitutive model was applied in seismic incremental dynamic analysis of a ten-floor steel frame and compared with the cyclic hardening model without considering damage and degradation. Meanwhile, the effects of damage and degradation on the seismic performance of steel frame were discussed in depth. The analysis results showed that: damages would lead to larger deformations. Therefore, when the calculated results of steel structures subjected to rare earthquake without considering damage were close to the collapse limit, the actual story drift of structure might already exceed the limit, leading to a certain security risk. ECM could simulate the damage and degradation behaviors of steel structures more accurately, and improve the calculation accuracy of traditional beam element model with acceptable computational efficiency.

Keywords: steel frame; equivalent constitutive model (ECM); degradation and damage; calculation models; nonlinear time history analysis; ABAQUS (UMAT)

1. Introduction

Due to the limited testing techniques and conditions, numerical calculation of elastic-plastic time history analysis widely used for predicting and simulating the seismic responses subjected to strong earthquake. The commonly used methods for nonlinear time history analysis of steel structures consist of shell or solid element model, multi-scale model and beam element model (Sivaselvan *et al*. 2000, Li and Feng 2000, Saatcioglu and Humar 2003, Liu and Zhang 2006,

*Corresponding author, Ph.D., E-mail: wangmeng1117@gmail.com
[a] Professor, Ph.D., E-mail: shiyj@mail.tsinghua.edu.cn
[b] Professor, Ph.D., E-mail: wang-yq@mail.tsinghua.edu.cn

http://www.techno-press.org/?journal=scs&subpage=8 ISSN: 1229-9367 (Print), 1598-6233 (Online)

Victor and Ernesto 2006, Motohide *et al*. 2007, Li *et al*. 2007, Krawinkler and Zareian 2007, Kuo *et al*. 2007). The shell or solid element model could describe more detailed constructions of structures, and also could obtain relatively accurate results of structure performances. However, the requirements for computing hardware and software conditions are too high to satisfy the computational demand and storage capacity. Although multi-scale model is more efficient than shell or solid element model, the problems of substantial computations and high storage costs are not solved yet. Therefore, the beam element model is still most commonly used in seismic analyses of whole structures, which can satisfy the computational requirements, and is convenient to obtain concerned internal forces. The disadvantages of traditional beam element models (bilinear model or trilinear model) are that they cannot describe the characteristics of local buckling and degradation caused by plastic strain accumulation under the earthquake, and cannot consider the reversible and irreversible features of structural damage. These problems will result in overestimating the structure collapse resistance, leading to a certain security risk.

Therefore, in reference (Wang *et al*. 2012b), author proposed an equivalent constitutive model of steel to simulate damage and degradation behaviors with beam element model, which was proved accurate and efficient by typical tests. The mathematical models were established to describe the responses of steel components and structures subjected to strong earthquake (as shown in Fig. 1), including the hysteretic skeleton curves, hysteretic criteria and degradation criteria. Further, the proposed model was implemented into the finite element software ABAQUS with its user subroutine interface (UMAT). Detailed comparisons between experimental curves and numerical results were made to verify the proposed model with a lot of component tests under static loadings (see the typical comparison results in Fig. 2 (Ricles *et al*. 2002 and Wang *et al*. 2011)).

In this paper, the static and dynamic tests of frame structures were adopted to verify the accuracy and application of equivalent constitutive model (ECM) (Wang *et al*. 2012b) in structural systems. Based on the verification, the computational accuracy and efficiency of shell element model, multi-scale model, ECM and bilinear model were compared by establishing four-story steel frame models with finite element software ABAQUS. The structural deformation, failure modes and the computational efficiency of different methods were also compared. Then,

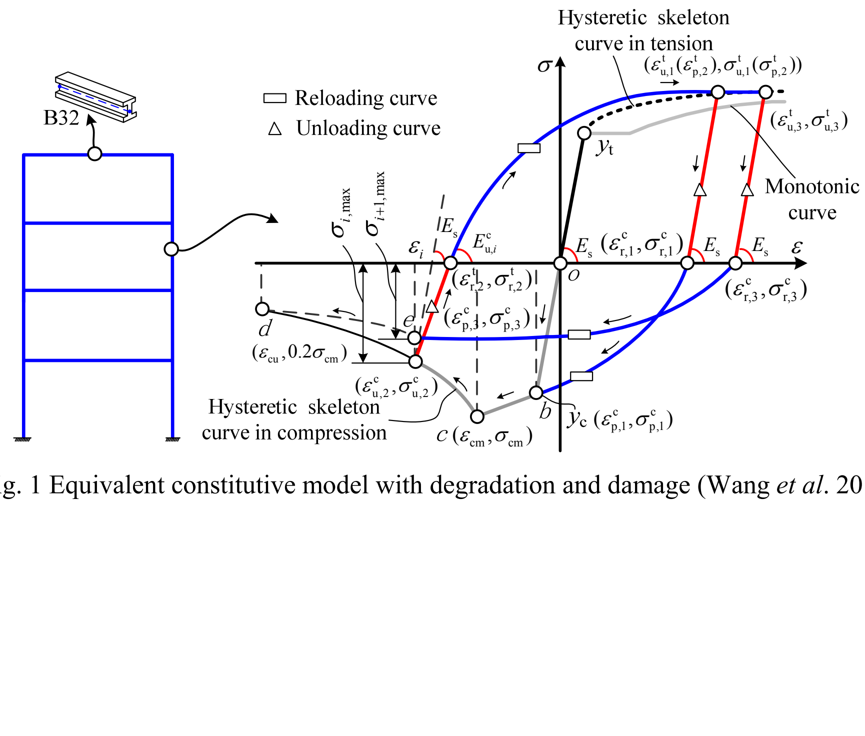

Fig. 1 Equivalent constitutive model with degradation and damage (Wang *et al*. 2012)

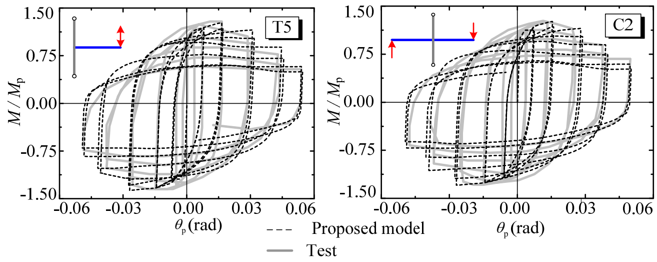

(a) Comparison analysis of reference (Ricles *et al*. 2002)

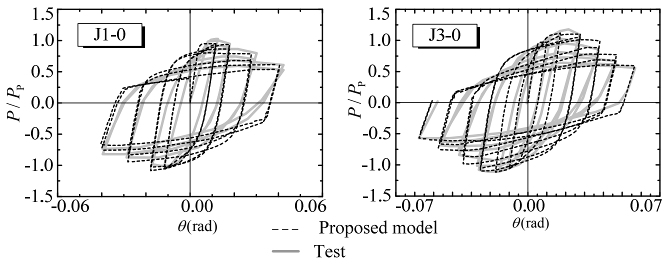

(b) Comparison analysis of reference (Wang *et al*. 2011)

Fig. 2 Comparison analysis of tests and ECM

the effects of damage and degradation on seismic performances of steel frame were discussed in depth. Finally, ECM was applied in seismic analysis of a ten-floor steel frame and compared with the cyclic hardening model without considering damage and degradation (Shi *et al*. 2011a). The primary incremental dynamic analysis was performed to further study the damage effect on the seismic behaviors of steel frame subjected to strong earthquake.

2. Numerical verification of ECM in steel frame structures

In order to verify the accuracy and applicability of equivalent constitutive model (ECM), the static tests and dynamic tests of frame structures were both selected. In this paper, the implicit dynamic analysis module of ABAQUS 6.9 (ABAQUS/Standard) was used as a computing platform for the time history analyses. B32 beam element in ABAQUS was adopted to establish frame models. B32 is a two-node three-dimension two-order Timoshenko beam element, which can allow for transverse shear deformation and satisfy the accuracy requirements of engineering. Six meshes were used for each beam to calculate. The proposed model was used based on user subroutine interface UMAT (User-defined Material Mechanical Behavior) for B32 with FORTRAN language. ABAQUS main program called the UMAT subroutine (the proposed model) at each material integration point before each load increment. The relative parameters were calculated by the mathematical expressions of damage control factors in reference (Wang *et al*. 2012b). The main influencing factors of damage and degradation behaviors included plate width-thickness ratio, the relative area ratio of flange and web, loading history and loading amplitude. Boundary conditions, lateral restraints and loading systems of finite element models were consistent with typical tests.

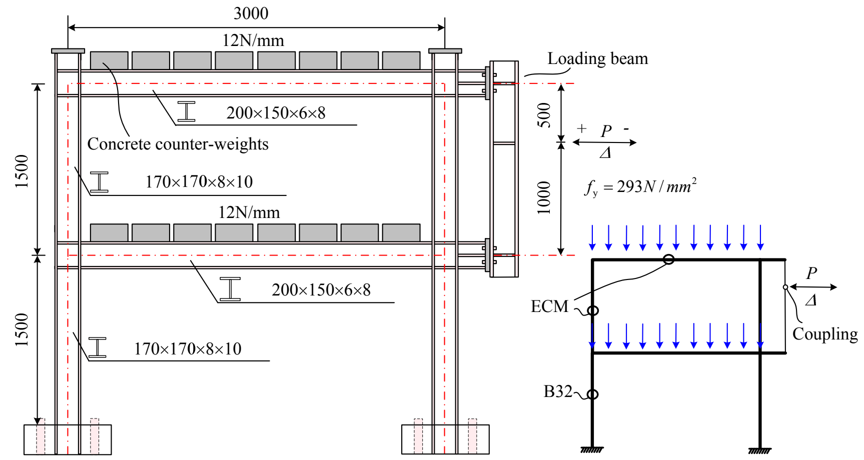

(a) Test description

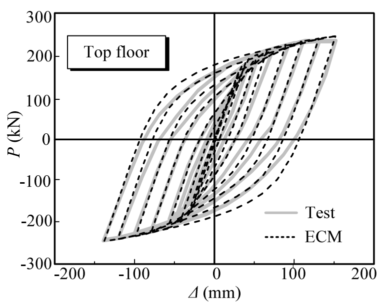

(b) Load-displacement curves of top floor

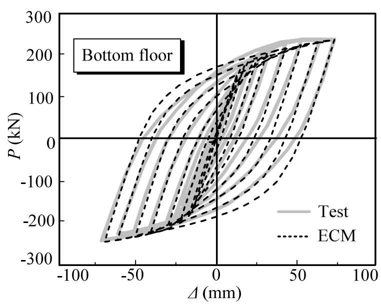

(c) Load-displacement curves of bottom floor

Fig. 3 Comparison analyses of tests and ECM of Guo *et al*. (2006)

2.1 The verification of ECM with static tests

Guo *et al*. (2006) carried out the 1:2 scale model tests of welded steel frame. Material properties, specimen sizes and loading devices were shown in Fig. 3(a). The beam element model was established in Fig. 3(a). The distributive beam was used for applying reciprocating displacements.

Load-displacement (P-Δ) curves of calculated results and tests were shown in Figs. 3(b) and (c). The calculated results with proposed model were satisfactory, while the calculated reloading curves were fuller than tests, which were related to the coefficients of proposed reloading curve.

2.2 The verification of ECM with nonlinear time history tests

In order to validate the equivalent constitutive model for time history analysis, the tests carried out by Kim *et al*. (2007) and Li *et al*. (2004) were adopted.

2.2.1 Test of Kim et al. (2007)

A two-story frame test of Kim *et al*. (2007) was selected. The material properties, specimen sizes and loading devices were shown in Fig. 4. The beam element model was established in Fig. 4.

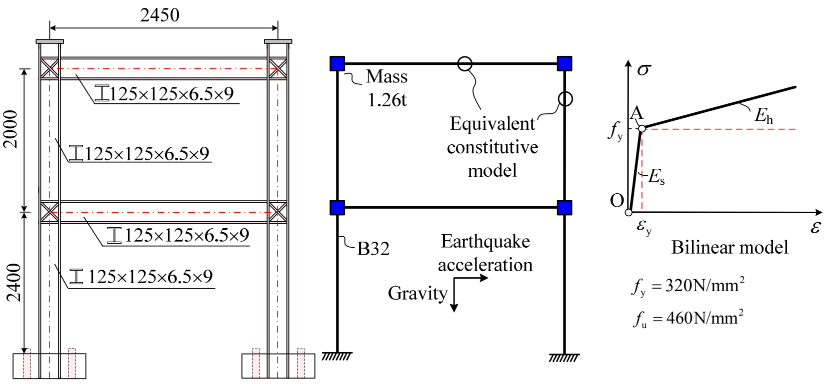

Fig. 4 Test description of Kim *et al*. (2007) (mm)

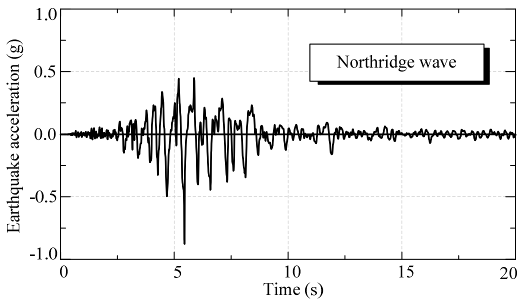

(a) Northridge wave (90055 Simi Valley-Katherine Rd)

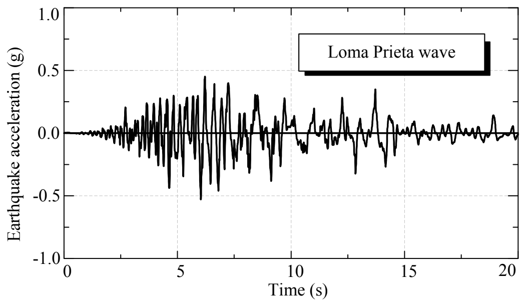

(b) Loma Prieta wave (47125 Capitola)

Fig. 5 Earthquake waves

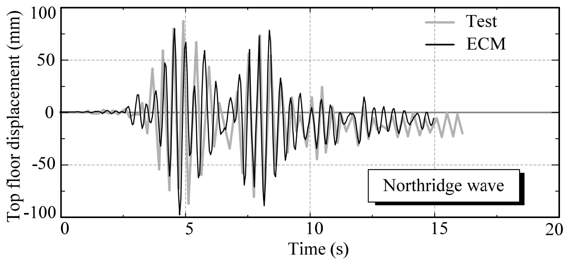

(a) Time history curves of top floor (ECM)

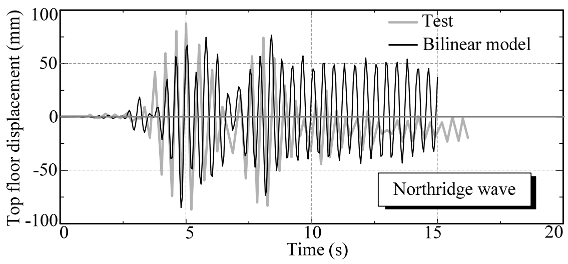

(b) Time history curves of top floor (Bilinear model)d

Fig. 6 Comparison analysis of experimental curves and calculated results (Northridge)

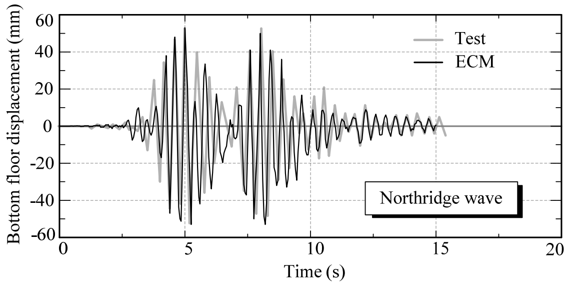

(c) Time history curves of bottom floor (ECM)

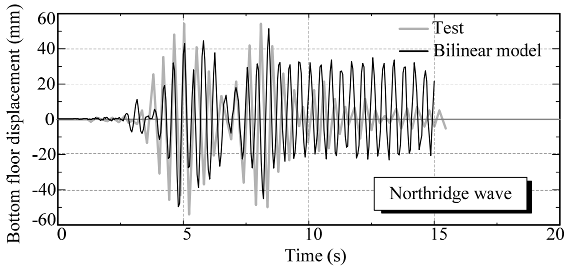

(d) Time history curves of bottom floor (Bilinear model)

Fig. 6 Continued

The X-stiffeners were fully welded at the panel zone to lessen shear deformation. A mass point of 1.26 t was imposed on each corner of frame. SS400 steel was used, and yield strength was 320 MPa. Northridge and Loma Prieta earthquake waves (Figs. 5(a) and (b)) were adopted, whose peak ground accelerations were 0.84 g and 0.53 g respectively. The finite element models were established with ECM and traditional bilinear model as constitutive models. Rayleigh damping was used in calculations. The damping ratio was determined as 2% according to Kim *et al*. (2007). The differences of calculated results of two models and the effects of damage and degradation on structures were discussed.

The calculated time history curves and the experimental curves of frames were compared in Figs. 6 and 7. The calculated results of ECM were in good agreement with actual curves, indicating the proposed model could better predict the peak displacement (the maximum difference was within 3.76%). The overall trends of time history curves were consistent with test results. The differences between calculated curves by ECM and the experimental curves may be caused by the differences of input seismic waves and the actual test waves. By contrast, bilinear model had larger differences from experimental results. The calculated peak displacement was relatively smaller than actual value, and in later stage, the model could not simulate the features of irreversible damage.

2.2.2 Test of Li et al. (2004)

The test model of reference (Li *et al*. 2004) was a one-span three-story steel frame structure. The size of the specimen was designed as 1:5 model of actual structure. The material was Q235 steel. The column was welded by steel plates of 3 mm thickness, and beam was No. 8 U-shaped steel. The beam was welded to the flange of column. The beam to column joint could be treated as

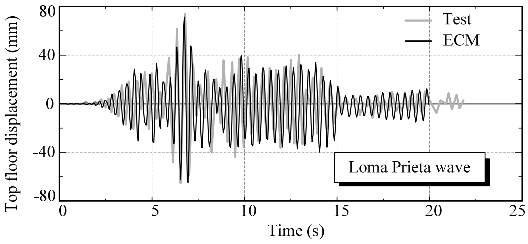

(a) Time history curves of top floor (ECM)

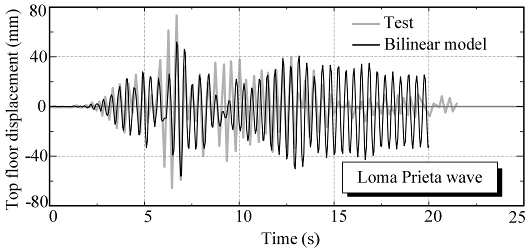

(b) Time history curves of top floor (Bilinear model)

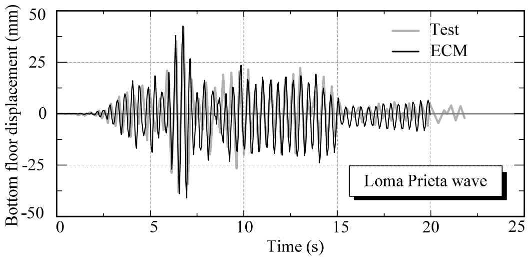

(c) Time history curves of bottom floor (ECM)

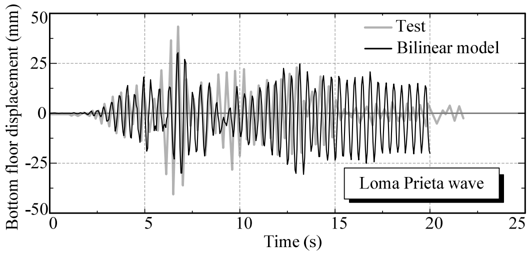

(d) Time history curves of bottom floor (Bilinear model)

Fig. 7 Comparison analysis of experimental curves and calculated results (Loma Prieta)

rigid connection. The specific dimensions and material properties were shown in Fig. 8(a). The slab was octagonal steel plate of 10 mm thickness, which was welded to the beams. The finite element model of plane frame was established instead of 3D model, because the seismic load was only imposed in one direction. The dead load of slab was applied as a concentrated load (mass point). The earthquake wave of El Centro the NS was input with peak acceleration of 0.7 g, as shown in Fig. 8(b). The constitutive models were respectively ECM and traditional bilinear model.

The calculated time history curves and the experimental curves of frame were compared in Figs.

8(c) and (d). The maximum seismic response absolute values of two models were compared in Table 1. The calculated results of ECM compared better with test results than bilinear model. Similar to the analysis of aforementioned test, the positions of calculated peak displacement were not consistent with tests, and the peak values were slightly higher than tests, because the differences of input seismic waves and the actual test waves could cause discrepant results.

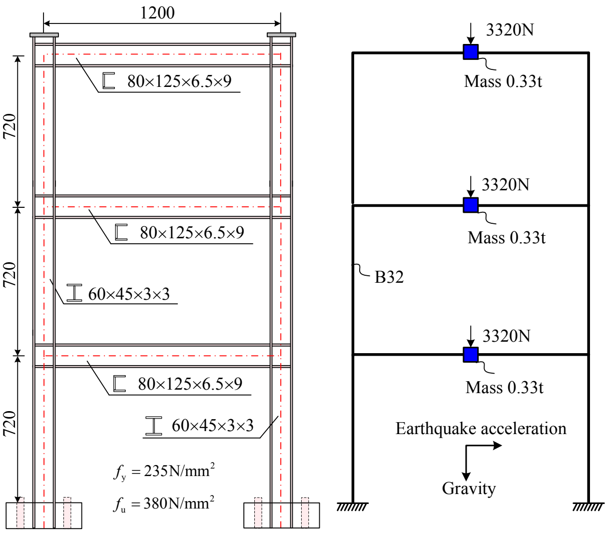

(a) Model description

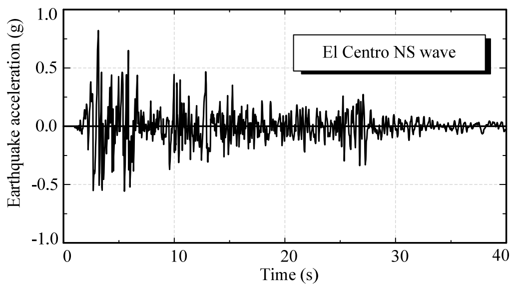

(b) El Centro NS wave

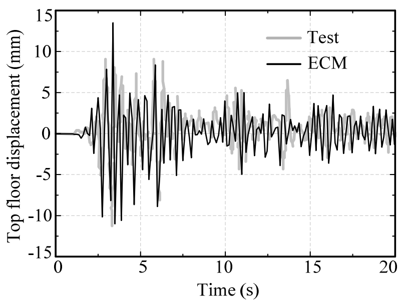

(c) Time history curves of top floor (ECM)

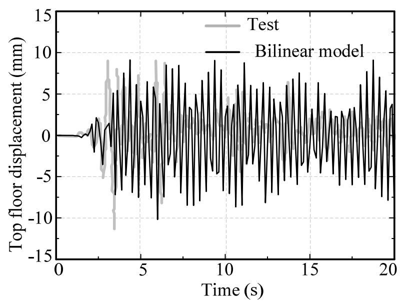

(d) Time history curves of top floor (Bilinear model)

Fig. 8 Comparison analysis of experimental curves and calculated results (test of Li *et al*. (2004))

Table 1 The comparison of maximum seismic response absolute values of two models

Waves	Position	Experiment	ECM	Bilinear model	ECM/Experiment
Northridge (Kim *et al*. 2007)	Top floor	90.32	98.21	83.46	1.09
	Second floor	53.40	52.87	49.65	0.99
Loma Prieta (Kim *et al*. 2007)	Top floor	71.35	70.23	56.78	0.98
	Second floor	42.06	43.25	29.39	1.03
El Centro (Li *et al*. 2004)	Top floor	12.15	13.62	10.03	1.14

In summary, the proposed equivalent constitutive model could well simulate the actual responses of steel frame structure and describe the degradation behaviors subjected to strong earthquakes, improving the computational accuracy of traditional beam element model.

3. The comparison of four models for time history analysis

3.1 Description of four models

In this paper, shell element model, multi-scale model, beam element model considering damage and degradation (ECM) and the traditional beam element model without considering damage and degradation were all established, as shown in Fig. 9. The different structural responses of time history analysis were calculated by these four models under strong earthquakes.

(1) Wang *et al*. (2012a, Journal of Building Structures) proved that the shell element model could well simulate the cumulative damage and degradation phenomenon caused by local buckling and plastic strain accumulation. The constitutive model used the hysteretic skeleton curve provided by reference (Shi *et al*. 2011a) (Fig. 10(a)). This method could predict the seismic responses more accurately based on the verification of tests.

(2) The constitutive model of beam element model considering damage and degradation was ECM. In terms of reference (Wang *et al*. 2012b) and the verification of shaking table tests in this paper, the proposed equivalent constitutive model (ECM) could well describe the strength and stiffness degradation of hysteretic curves by introducing the damage factors into material constitutive model, as shown in Fig. 1.

(3) The traditional beam element model is the most commonly used for calculating structural responses with kinematic hardening criterion. The steel material properties were simplified with a simple bilinear form, as shown in Fig. 10(b). However, this model did not consider the cyclic hardening characteristics and the degradation phenomenon.

(4) The multi-scale simulation is a rapidly developing hot method, which has been widely used in many fields. It is a balanced solution between computational accuracy and computational cost. Shell element model or solid element model (three-dimension model) is used for establishing details of structural connections, bolts and other parts with complex stress state, while beam element model (one-dimension model) is used for beam and column of frame, as shown in Fig. 11. The effective connection interface of three-dimension model and one-dimension model is prerequisite for multi-scale analysis. In terms of cooperative work between different scale parts, the multi-scale combination of

complex connection and simplified beam and column is achieved in Fig. 11. The "Couple" command in "Interaction" module of ABAQUS is used for the deformation compatibility of contact surfaces. In multi-scale model, the constitutive model of shell element model is the hysteretic skeleton curve in Fig. 10(a), and the constitutive model of beam element model is bilinear curve in Fig. 10(b). The connection method of different scale parts was proved reliable in reference (Shi and Wang 2011b, Engineering Mechanics). Taking the test of Castiglioni and Pucinotti (2009) for example, the specific dimensions of the specimen and loading device were shown in Fig. 12(a). The calculated curves of multi-scale model and shell element model were consistent with test results in Fig. 12(b). Serious local buckling resulted in obvious degradation of hysteretic curves (Fig. 12(a)), which could not be simulated by traditional beam element models.

By using above-mentioned four models, elastic-plastic time history analyses were carried out. The calculated deformations were compared. The computational accuracy and efficiency of different methods were discussed. Then, the effects of damage and degradation on seismic responses of structures were investigated.

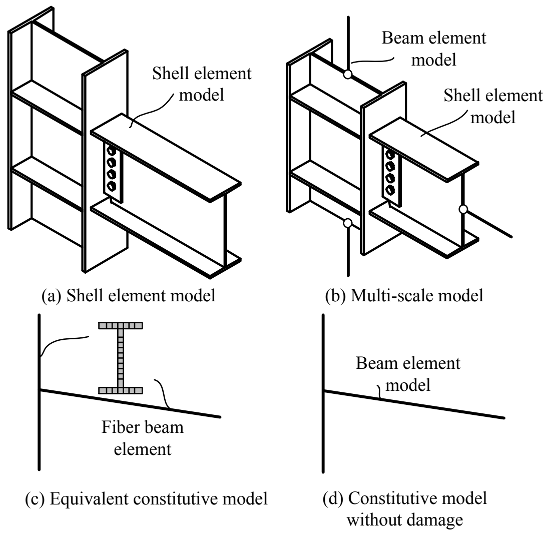

Fig. 9 The widely used models for time history analyses

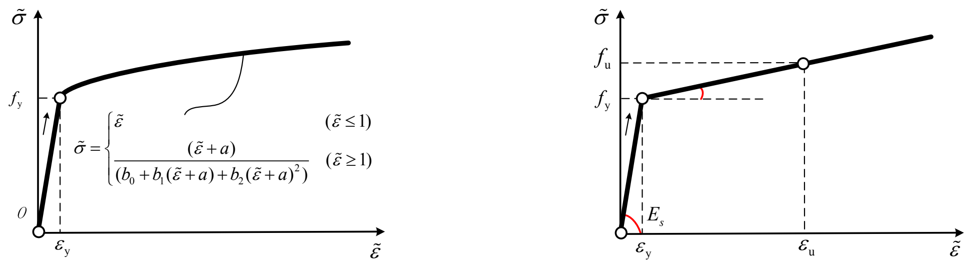

(a) Hysteretic skeleton curve (Shi *et al*. 2011a) (b) Bilinear model

Fig. 10 Constitutive models

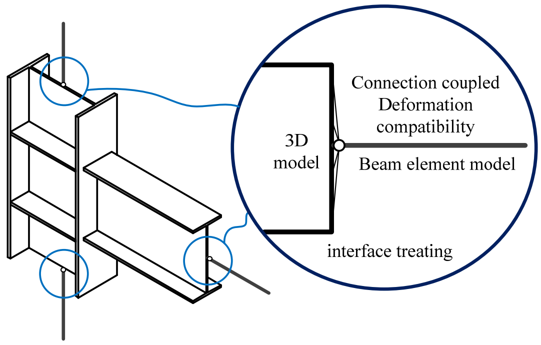

Fig. 11 The effective connection method of different scale parts

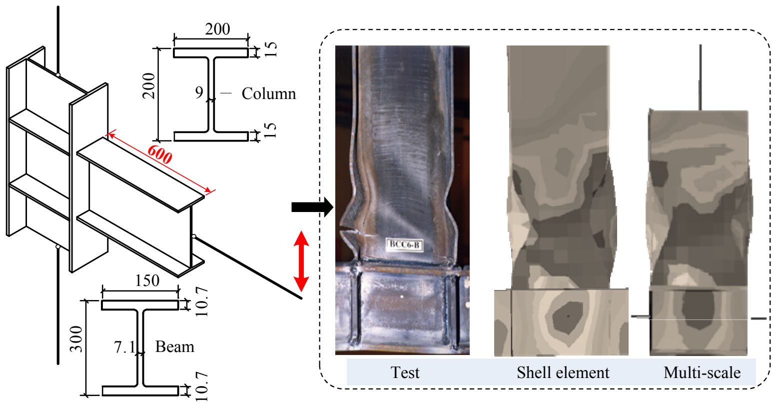

(a) Model description and comparison analysis of typical failure modes

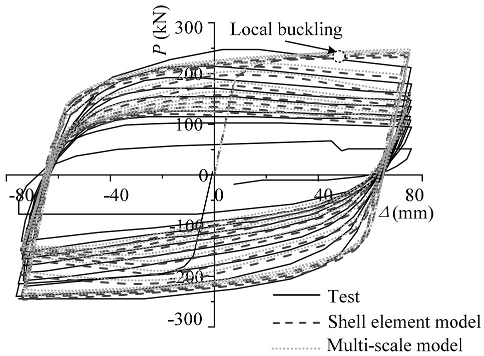

(b) Comparison analysis of hysteretic curves (Castiglioni and Pucinotti 2009)

Fig. 12 Experimental verification of multi-scale model

3.2 Calculation parameters

Four-story steel frame models with one span were designed as shown in Fig. 13. The story height was 3000 mm and span was 6000 mm. Traditional beam element model, beam element model considering damage and degradation, multi-scale model and shell element model were

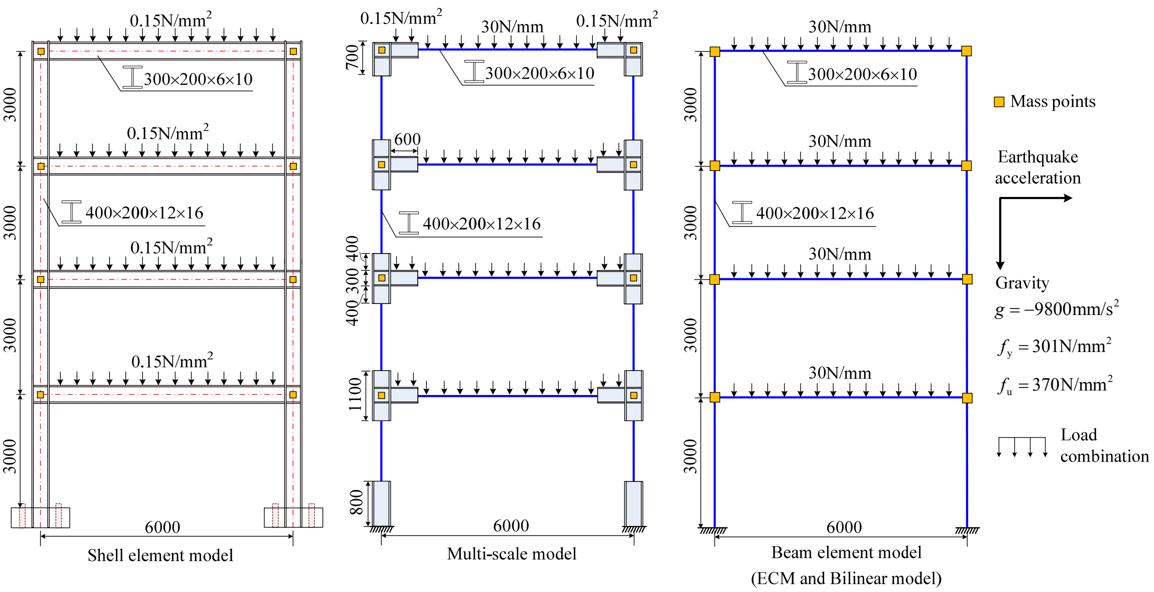

Fig. 13 Model description

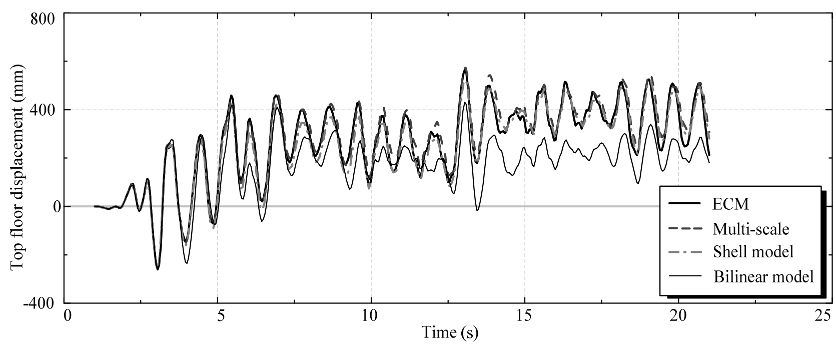

(a) El Centro NS wave

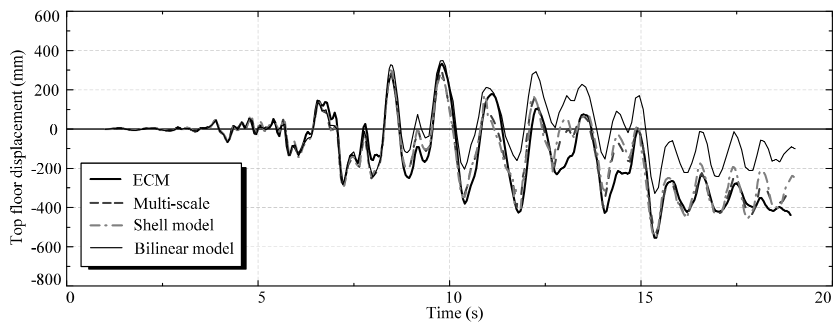

(b) Loma Prieta wave

Fig. 14 Comparison of top floor displacement of four models respectively established in ABAQUS. Beam element model was the axes of shell element model. In multi-scale model, the shell elements were used at the positions of beam-to-column connections and column foots, where local buckling was more able to occur. In beam-to-column connection region, the length of beam with shell element was taken as twice of beam height, and the length of column with shell element was taken as one time of column height. The length of column foot with shell element was twice of column height. According to the principle of "strong column and weak beam" (GB50011-2001), the beam-to-column connections were designed relatively strong, which could be considered as rigid connection with small shear deformation. Lateral restraint of beams was applied to prevent overall instability. Column foots were rigidly connected. Detailed dimensions of model and material parameters were shown in Fig. 13. The constitutive relations adopted the models described in Section 3.1. The parameters of ECM were obtained according to reference (Wang *et al*. 2012b).

To carry out time history analyses with four models, the first step was to impose gravity load and the combination of constant loads and live loads on the structures required by GB50009-2001. The surface loads or line loads were separately applied on different models. The representative values of gravity load were imposed as mass points on beam ends. The second step was to input ground motion acceleration records to the structures, and the elastic-plastic time-history analyses were then carried out to investigate the differences of structural seismic responses calculated by different models. El Centro NS and Loma Prieta earthquake records were selected, as shown in Fig. 8(b) and 5(b). The PGA (peak ground acceleration) values were 0.82 g and 0.63 g respectively. In order to study the impact of cumulative damage on structure and the degraded responses of frame under a severe earthquake, the PGA was adjusted to 1.0 g considering highly non-linear behaviors of geometry and material.

3.3 Results analysis

The calculated time history displacement curves of four models were compared, as shown in Fig. 14. Before the damage occurred, the curves of four models were consistent, indicating that the established four models were basically equivalent in elastic stage. Once the damage occurred, the calculated results of the models considering damage were different from the model without damage. The probable reasons were that if the plastic strains were accumulated to a certain value, obvious plastic hinges were formed at the beam end and column foot of shell element model and multi-scale mode (overall and local deformations in Figs. 15(a) and (b)), resulting in irreversible damage and degradation of structures. The unrecoverable deformation and degraded stiffness caused the redistribution of internal forces, and the deformations were continuously accumulated in one side. Therefore, ECM considered the damage and degradation behaviors, so it could predict the real responses of structure more accurately subjected to strong earthquake and obtain the amplification effects of damage on structural deformations. From the comparison curves in Fig. 14, the results of ECM, shell element model and multi-scale model were basically the same, and deformation distributive forms of three models were coincident. On the contrary, the calculated deformations of traditional bilinear model without considering damage and degradation were relatively smaller than the other three models, and it overestimated the collapse resistance of the structure, leading to unsafe design.

From the distribution curves in Figs. 16 and 17, the positions of weak layers of four models were basically the same, and four models had similar predictions for the distribution of inter-story drift ratio. However, the calculated deformations of bilinear model were significantly smaller than

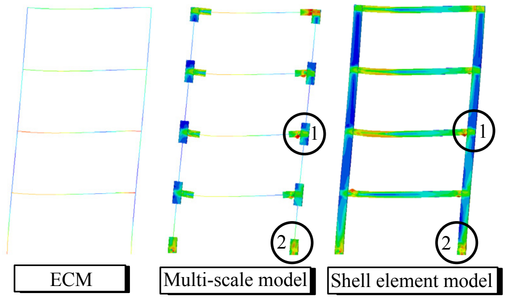

(a) Overall deformation

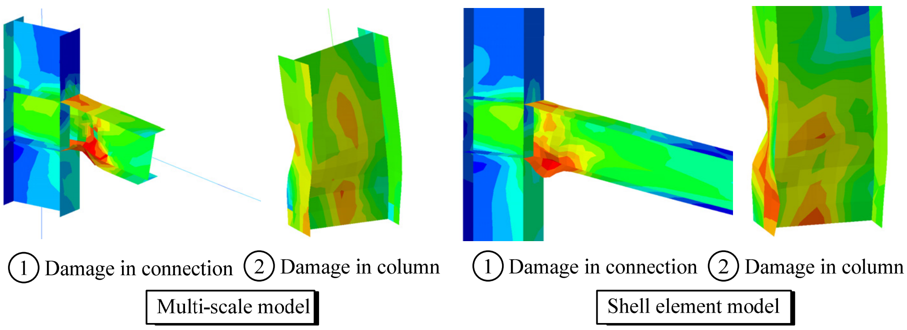

(b) Local damage and failure modes

Fig. 15 Failure modes

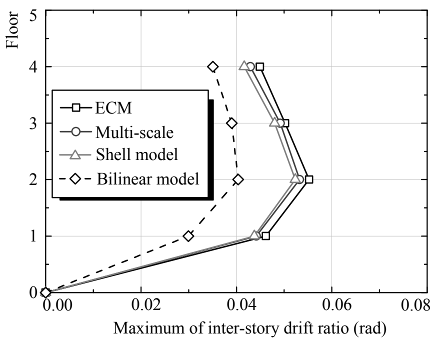

(a)

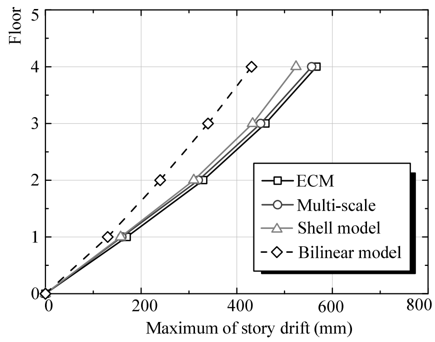

(b)

Fig. 16 Maximum of structure deformation (El Centro NS wave)

the other three models, indicating that the traditional beam element model underestimated the structure deformations without considering the cumulative damage impact on structures. Damage would lead to larger deformations. Therefore, when the calculated results of steel structures subjected to rare earthquake without considering damage were close to the collapse limit, the actual story drift of structure might already exceed the limit, leading to potential hazards. Though the results of ECM model were slightly larger than the other models, the difference was within the acceptable range and these results were safe for design.

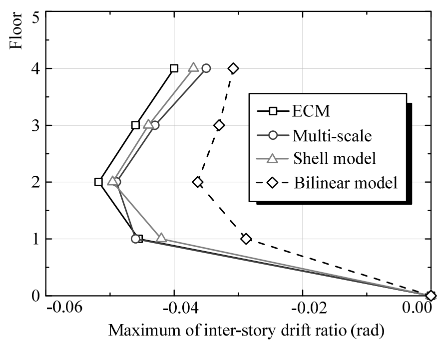

(a)

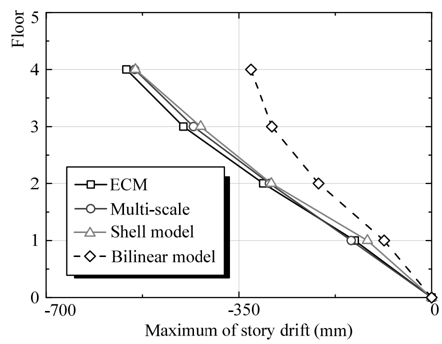

(b)

Fig. 17 Maximum of structure deformation (Loma Prieta wave)

Table 2 Computing time of seismic response of three types (min)

Input earthquake wave	El Centro NS wave	Loma Prieta wave
Shell element model	504	431
Multi-scale model	267	241
ECM	165	177
Bilinear model	152	145

The computational efficiency of four models was summarized in Table 2. Although the time of bilinear model was the least, its accuracy was inferior to the other three models. The Beam element model considering damage (ECM) could guarantee the accuracy and significantly reduce the computation time. It was an equilibrium solution between accuracy and computational cost. With the increasing number of elements, its superiority will be more remarkable.

4. Application of ECM in steel frame analysis

4.1 Basic parameters

In order to investigate the effects of cumulative damage and degradation on seismic behaviors of actual steel frame, a ten-story frame model was established with beam element in Fig. 18 for nonlinear time history analysis. The height of each story was 3200 mm and the length of each span was specified as 6450 mm. Beam and column sizes were shown in Fig. 18(a), and the size of bottom column section was enlarged according to actual situation. Due to the principle of “strong column and weak beam” (GB50011-2001), the beam-to-column joint could be treated as rigid connection with its small shear deformation. In order to prevent the overall instability, lateral constraints were applied to simulate the restraints provided by beams out of plane. Calculations were carried out respectively using cyclic hardening model without considering damage and degradation (Shi *et al*. 2011a) (described in Fig. 18(c)) and equivalent constitutive model (ECM) considering damage and degradation (Fig. 1). The cyclic hardening model was proved accurate for simulating the cyclic behaviors of steel material in reference (Shi *et al*. 2011a). Here, the cyclic hardening parameters of Q235B steel were used. The parameters of ECM were obtained according to reference (Wang *et al*. 2012b). Incremental dynamic analyses were carried out. The first step was to apply vertical gravity loads and the load combination on the structure according to reference (JGJ 101-96). For seismic analysis, the representative values of gravity load should be imposed as mass points on beams. The second step was to input ground motion acceleration to the structure in horizontal direction. Three earthquake waves were selected, including El the Centro earthquake wave (Fig. 8(b)), Koyna earthquake wave (Fig. 17(b)) and the Northridge earthquake

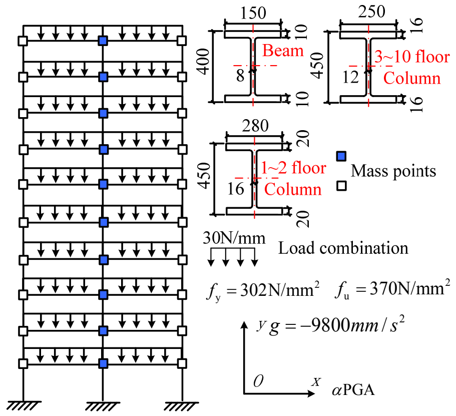

(a) Specimen details (mm)

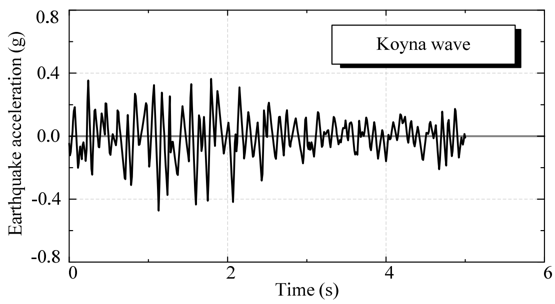

(b) Koyna earthquake waves (mm)

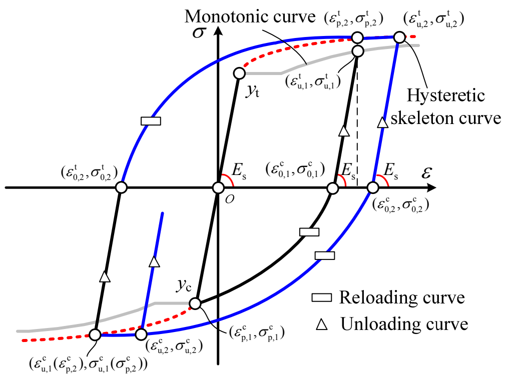

(c) The cyclic hardening model without damage and degradation (Shi *et al*. 2011)

Fig. 18 Model description

Table 3 Loading patterns

Waves	Scale factor of peak acceleration (PGA) is α				
	(0.4)	(1.0)	(1.5)	(1.9)	(2.2)
El Centro	A	B	C		
Koyna	A	B	C	D	
Northridge	A	B	C	D	E

wave (Fig. 5(a)). The PGA value of El Centro earthquake wave was 0.82 g, 0.63 g for the Koyna earthquake wave and 0.74 g for Northridge earthquake wave. In order to study the impact of cumulative damage on the structure, α PGA of three seismic waves were input (where, α is the scale factor, as shown in Table 3). The starting of the latter stage was the end of the former stage, and the peak accelerations were gradually increased to investigate the structural responses under different seismic intensities.

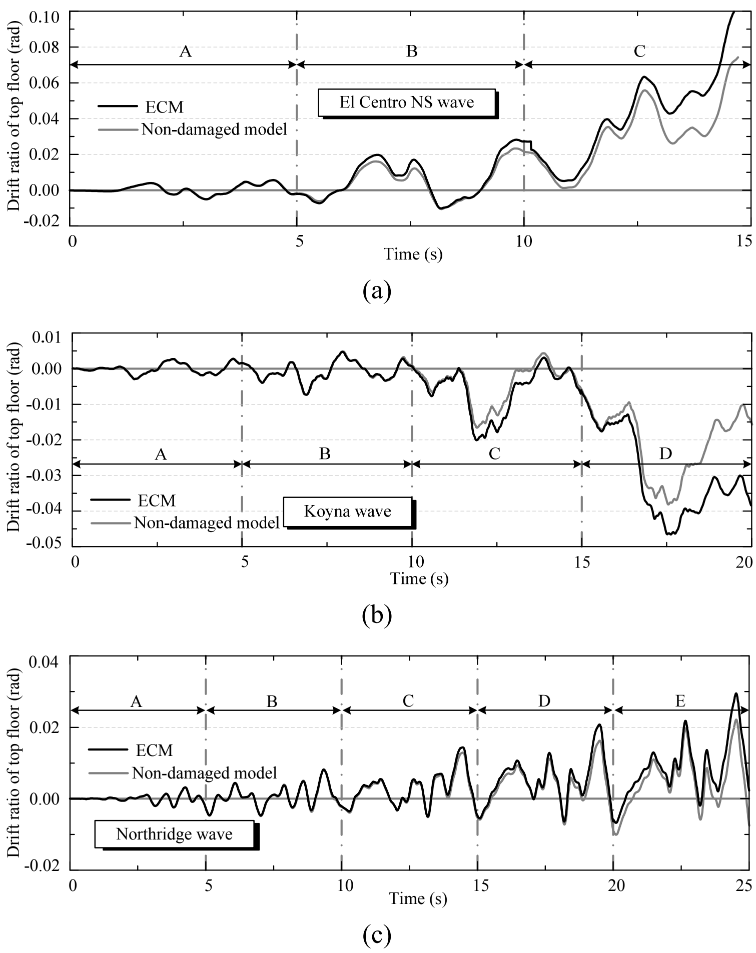

(a)

(b)

(c)

Fig. 19 Comparison of drift ratio of top floor

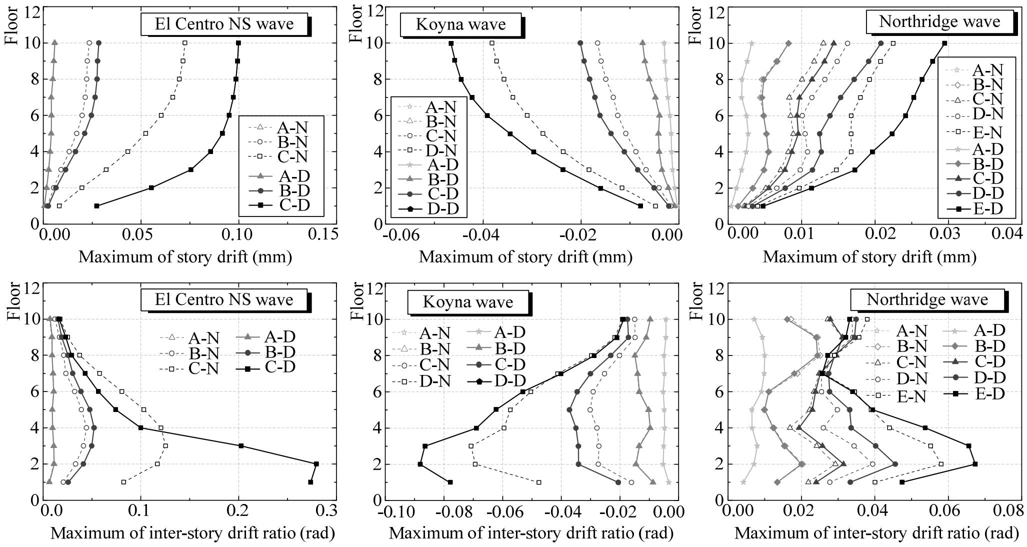

Fig. 20 Comparison of structure deformations

4.2 The calculated results of time history analysis

The calculated displacement curves, the maximum inter-story drift ratios and the maximum drift distributions of two models were shown in Figs. 19 and 20. Actually, under strong earthquake, the plastic strain accumulation and local buckling phenomenon occurred in column foots and beam ends. These phenomena could not be simulated by the beam element model without considering damage and degradation. It could be seen from the distribution curves in Fig. 19 that before the damage occurred, the curves of two models were consistent, while once the damage occurred, the curves were obviously different. The calculated results of the damage model were significantly larger than non-damage model due to accumulated degradation. Because of the irreversible and unrecoverable damage, the calculated displacement of damage model became gradually diverging. The differences of two curves showed that the model without considering damage and degradation would overestimate the collapse resistance of structure, leading to insecurity of design.

From the comparison analyses of distribution curves in Fig. 20, the calculated results of non-damage model (cyclic hardening model X-N) were smaller than the one of damage model (ECM X-D), and the maximum differences would be more than 30%. The locations of weak layers were basically concentrated in 2 to 4 floors. Strong seismic waves made the structure deformation more asymmetric. Then, the residual deformations were continuously accumulated in one side of the structure, leading to gradual increase of the drift ratio and the top floor displacement. With the continuous increasing of peak acceleration, the damage got more serious, and the residual deformation became larger, then the differences of calculated curves by two models became more obvious. The damage degrees of different earthquake waves were not the same due to different loading patterns and different process of cumulative deformations.

4.3 Incremental dynamic analysis curves

The primary curves of incremental dynamic analysis were obtained by extracting the maximum

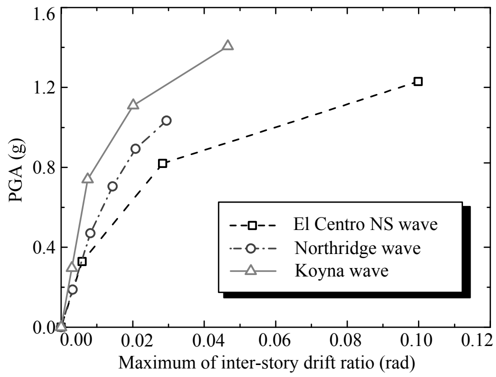

Fig. 21 Incremental dynamic analysis curves

displacements of different accelerations under different earthquake waves, as shown in Fig. 21. This curve was characterized by the capacity demand and collapse resistance of structure subjected to various magnitudes of earthquakes. It better described the changing process of stiffness, strength and deformation capacity of structure under dynamic loadings, and could obtain the changing nonlinear dynamic responses of structure. Incremental dynamic analysis curves could reasonably reflect the damage and degradation phenomenon of structure resistance subjected to dynamic excitations, while the curves of different waves were quite different.

5. Conclusions

Based on the proposed model in reference (Wang *et al.* 2012b), the equivalent constitutive model was applied in the static and dynamic frame tests. The computational accuracy and efficiency of shell element model, multi-scale model, ECM and traditional beam element model were compared by establishing four-story steel frame models using finite element software ABAQUS. Finally, the ten-story steel frame models were established with ECM and cyclic hardening model without considering damage (Shi *et al.* 2011a). The Incremental dynamic analysis was carried out to investigate the effect of damage and degradation on the structure. The main conclusions could be drawn as follow:

(1) Equivalent constitutive model can simulate the static and dynamic characteristics of steel structures accurately. The model improved the computational accuracy of traditional beam element model.
(2) Before the damage occurred, the curves of four models were consistent. Once the damage occurred, the results of ECM, shell element model and multi-scale model were basically the same, indicating that ECM could more accurately predict the amplification effect of damage on structure deformation. The results of traditional beam element model without considering damage and degradation were relatively smaller than the other three models. Therefore, when the calculated results of steel structures subjected to rare earthquake without considering damage were close to the collapse limit, the actual story drift of structure might already exceed the limit, leading to a certain security risk.
(3) For computational efficiency, the calculation time of ECM was far less than shell element model and multi-scale model, and a little more than bilinear model. ECM was a balanced

solution between accuracy and computational cost.

(4) Due to the irreversible and unrecoverable behaviors of damage, the calculated results of non-damage model were smaller than damage model, and the maximum differences could be more than 30%. Therefore, if the damage and degradation behaviors were not considered in design, the collapse resistance of the structure would be overestimated, leading to insecurity of design. The incremental dynamic analysis curves could estimate the dynamic resistance of the overall structure and describe the resistance degradation of structure under dynamic excitations reasonably. However, the curves of different waves were quite different.

Acknowledgments

This work described in paper was supported by National Natural Science Foundation Grant (No. 51408031), Beijing Natural Science Foundation (No. 8154052) and Fundamental Research Funds of Central Universities (2014JBM074).

References

ABAQUS (2009), "Analysis user's manual I_V. Version 6.9", ABAQUS, Inc., Dassault Systèmes, USA.

Ballio, G., Calado, L. and Castiglioni, C.A. (1997), "Low cycle fatigue behaviour of structural steel members and connections", *Fatig. Fract. Eng. Mater. Struct.*, **20**(8), 1129-1146.

Castiglioni, C.A. and Pucinotti, R. (2009), "Failure criteria and cumulative damage models for steel components under cyclic loading", *J. Construct. Steel Res.*, **65**(4), 751-765.

Guo, B., Guo, Y.L. and Liu, F. (2006), "Research on cyclic behavior of welded and bolted steel frames", *J. Build. Struct.*, **27**(2), 47-56.

Li, G.Q. and Feng, J. (2000), "A practical approach for estimating elasto-plastic displacements of multistory and tall steel buildings under severe earthquakes", *J. Build. Struct.*, **21**(1), 77-83.

Li, H.Q., Ben, Q.G., Yu, Z.H., Zhang, Y.Q. and Lu, X.L. (2004), "Analysis and experiment of cumulated damage of steel frame structures under earthquake action", *J. Build. Struct.*, **25**(3), 69-74.

Li, Z.X., Sun, Z.H., Guo, L., Chan, H.T. and Yu, Y. (2007), "Concurrent multi-scale modeling of structures and damage analyses", *J. Southeast Univ.* (*Natural Science Ed.*), **37**(2), 251-260.

Liu, Y.H. and Zhang, Y.C. (2006), "Refined plastic hinge analysis of spatial steel frames", *Eng. Mech.*, **23**(sup. I), 108-116.

Kim, S.E., Lee, D.H. and Cuong, N.H. (2007), "Shaking table tests of a two-story un-braced steel frame", *J. Construct. Steel Res.*, **63**(3), 412-421.

Krawinkler, H. and Zareian, F. (2007), "Predication of collapse-how realistic and practical is it and what can we learn from it?", *Struct. Des. Tall Special Build.*, **16**(5), 633-653.

Kuo, W.L., Yi, K.W. and Foutch, D.A. (2007), "Evaluation of 3D steel moment frames under earthquake excitations. I: Modeling", *J. Struct. Eng.*, **133**(3), 462-470.

Ministry of Housing and Urban-Rural Development of the People's Republic of China (2010), GB50011-2010 Code for Seismic Design of Buildings; Beijing, China Architecture & Building Press.

Ministry of Housing and Urban-Rural Development of the People's Republic of China (1997), JGJ 101-96 Specificating of Testing Methods for Earthquake Resistant Building; Beijing, China Architecture & Building Press.

Motohide, T., Makoto, O., Satoshi, Y., Shojiro, M. and Kazuhiko, K. (2007), "E-defense tests on full-scale steel buildings Part 3 - Analytical simulation of collapse", *Proceedings of ASCE Structures Congress*, Long Beach, CA, USA, May.

Ricles, J.M., Mao, C.S., Lu, L.W. and Fisher, J. (2002), "Inelastic cyclic testing of welded unreinforced

moment connections", *J. Struct. Eng.*, **128**(4), 429-440.
Saatcioglu, M. and Humar, J. (2003), "Dynamic analysis of buildings for earthquake resistant design", *Can. J. Civil Eng.*, **30**(2), 338-359.
Shi, Y.J., Wang, M. and Wang, Y.Q. (2011a), "Experimental and constitutive model study of structural steel under cyclic loading", *J. Construct. Steel Res.*, **67**(8), 1185-1197.
Shi, Y.J., Wang, M. and Wang, Y.Q. (2011b), "Seismic behavior analysis of steel frame by multi-scale calculation method", *Eng. Mech.*, **28**(12), 20-26.
Sivaselvan, M.V. and Reinhorn, A.M. (2000), "Hysteretic models for deteriorating inelastic structures", *J. Eng. Mech.*, **126**(6), 633-640.
Victor, I.F. and Ernesto, F.C. (2006), "Parametric study of the non-linear seismic response of three-dimensional building models", *Eng. Struct.*, **28**(5), 756-770.
Wang, W., Zhang, Y.Y., Chen, Y.Y., Lu, Z.H. and Yan, P. (2011), "Improving seismic performance of steel moment connections with noncompact beam web", *Proceedings of the 6th International Symposium on Steel Structures*, Seoul, Korea, November, pp. 517-522.
Wang, M., Shi, Y.J. and Wang, Y.Q. (2012a), "Effect of damage and degradation on steel frame seismic behaviors under severe earthquake", *J. Build. Struct.*, **33**(10), 94-101.
Wang, M., Shi, Y.J. and Wang, Y.Q. (2012b), "Equivalent constitutive model of steel with cumulative degradation and damage", *J. Construct. Steel Res.*, **79**(10), 101-114.

BU

Notation

The following symbols are used in this paper

E_s	Young's modulus
E_s	Hardening modulus
f_y	yield stress in tension
ε_y	yield strain in tension
f_u	ultimate stress
α	Scale factor of peak acceleration (PGA)
P	the reaction force of the beam tip
P_y	yield load
Δ	the imposed displacement of the beam tip
M	moment of beam root
M_y	yield moment of beam root
M_p	plastic moment of beam section